HHS Public Access

Author manuscript

Vaccine. Author manuscript; available in PMC 2016 September 22.

Published in final edited form as:

Vaccine. 2015 September 22; 33(39): 5064–5071. doi:10.1016/j.vaccine.2015.08.025.

Nanovaccines for Malaria Using *Plasmodium falciparum* Antigen Pfs25 Attached Gold Nanoparticles

Rajesh Kumar[a], **Paresh C. Ray**[b], **Dibyadyuti Datta**[a], **Geetha P. Bansal**[a], **Evelina Angov**[c], and **Nirbhay Kumar**[a,d]

[a]Department of Tropical Medicine and Vector-Borne Infectious Diseases Research Center, School of Public Health and Tropical Medicine, Tulane University, New Orleans, LA 70112

[b]Department of Chemistry and Biochemistry, Jackson State University, Jackson, MI 39217

[c]Walter Reed Army Institute for Research, Silver Spring, MD

Abstract

Malaria transmission-blocking vaccines (TBV) targeting sexual stages of the parasite represent an ideal intervention to reduce the burden of the disease and eventual elimination at the population level in endemic regions. Immune responses against sexual stage antigens impair the development of parasite inside the mosquitoes. Target antigens identified in *Plasmodium falciparum* include surface proteins Pfs230 and Pfs48/45 in male and female gametocytes and Pfs25 expressed in zygotes and ookinetes. The latter has undergone extensive evaluation in pre-clinical and phase I clinical trials and remains one of the leading target antigens for the development of TBV. Pfs25 has a complex tertiary structure characterized by four EGF-like repeat motifs formed by 11 disulfide bonds, and it has been rather difficult to obtain Pfs25 as a homogenous product in native conformation in any heterologous expression system. Recently, we have reported expression of codon-harmonized recombinant Pfs25 in *E. coli* (CHrPfs25) and which elicited highly potent malaria transmission-blocking antibodies in mice. In the current study, we investigated CHrPfs25 along with gold nanoparticles of different shapes, size and physicochemical properties as adjuvants for induction of transmission blocking immunity. The results revealed that CHrPfs25 delivered with various gold nanoparticles elicited strong transmission blocking antibodies and suggested that gold nanoparticles based formulations can be developed as nanovaccines to enhance the immunogenicity of vaccine antigens.

1. Introduction

Malaria caused by *Plasmodium* spp. remains a major public health problem, responsible for up to an estimated 283 million cases and 755,000 deaths annually (WHO, 2014). Widespread drug resistance (1) (2), and lack of appropriate means of disease control underscore the need for developing effective vaccines targeting different stages of the

[d]Corresponding author (nkumar@tulane.edu, 504-988-2577-Tel).

parasite life cycle. The only vaccine advanced to phase III clinical trial (RTS, S/AS01) has shown only partial efficacy (3, 4).

Malaria transmission-blocking vaccine (TBV) targeting sexual stages of the parasite represents an ideal intervention to reduce the burden of the disease by controlling vector mediated transmission and eventual elimination at the population level in endemic areas (5–10). Immune responses against sexual stage antigens impair the development of parasite inside the mosquitoes, thus, curtailing the transmission. *P. falciparum* proteins Pfs230 (11–17), Pfs48/45 (18–20) and Pfs25 (21–25) and their orthologs in *P. vivax* are primary target antigens for TBVs. Of these target antigens, Pfs25 expressed on the surface of zygotes and ookinetes, has undergone extensive evaluation in pre-clinical and phase I clinical trials and remains one of the promising target antigens for the development of TBV. Several studies have reported on the recombinant expression of Pfs25 in yeast (22), cell-free translation using wheat germ(26), plants (14) and algae (27) with varying degrees of transmission-blocking effectiveness in pre-clinical studies (28–31) and phase I clinical trials (32). Since Pfs25 has a complex tertiary structure characterized by 22 conserved cysteine residues critical for structural integrity of the antigen, it has been rather difficult to produce in native conformation in any heterologous expression system (33, 34). Recently, we have reported expression of codon-harmonized recombinant Pfs25 (CHrPfs25) in *E. coli* and the successful refolding and purification in an appropriate monomeric conformation, which elicited highly potent malaria transmission-blocking antibodies in mice (24).

To be an effective vaccine an antigen formulation has to induce strong and preferably long-lasting antibody responses (35). Immune responses are modulated by incorporation of effective adjuvants, optimization of delivery systems and fine-tuning of vaccine particulate size. However, the development of vaccines in general, has been hindered by the paucity of safe and effective vaccine adjuvants and delivery systems. Several studies have shown that antigen delivery with nanoparticles could enhance the uptake of antigen by antigen presenting cells and subsequently elicit improved immune response than those obtained with soluble counterparts (36, 37). In this regard, gold nano-(GN)-particles may serve as efficient and cost-effective approach for vaccine delivery because of their tunable particle size, shape, biocompatibility, unique physicochemical properties, and easy surface modifications (38–44). GN-particles are inert, non-toxic, and can be easily taken up by dendritic cells and other antigen presenting cells facilitating overall improved delivery of vaccine antigen (40, 41, 45, 46). Despite the huge potential benefit of GN-particles in the field of biomedical imaging and diagnostics, only a few studies have reported on delivery of vaccine antigens (47, 48).

In the current study, we have investigated GN-particles of different shapes and size, and evaluated their potential for delivery of CHrPfs25 antigen for induction of transmission blocking immunity. The efficacy of GN-particles for induction of transmission blocking antibodies was also determined when co-administered with conventional adjuvant alum. The results revealed that CHrPfs25 delivered with GN-particles elicited strong transmission blocking antibodies, and suggested that GN-particles can be developed as promising vaccine delivery vehicles to enhance the immunogenicity of vaccine antigens.

2. Methods

2.1. Purification of CHrPfs25

The CHrPfs25 protein was expressed in *E. coli* and purified after refolding as described (24). The quality of protein was analyzed by non-reducing and reducing denaturing SDS-PAGE and characterized by western blot analysis using anti-$(His)_6$ and Pfs25-specific monoclonal (ID3) antibodies (24). The concentration of protein was determined by BCA protein assay kit (Thermo Scientific, Rockford, IL). Endotoxin levels were measured using LAL chromogenic endotoxin quantitation kit (Thermo Scientific, Rockford, IL) and were found to range between 0.7 and 7.2 EU/mL in three different batches of CH-rPfs25 employed for further formulation with gold nanoparticles in these studies. These levels are significantly lower than maximum acceptable levels of endotoxin in vaccine formulation during preclinical research(49).

2.2. Nanoparticle synthesis and bio-conjugation

GN-particles of different shapes were chemically synthesized as described (50–55). To synthesize spherical GN-particles (GNP, Figure 1A) (53, 55), aqueous solutions of $HAuCl4.3H_2O$ (1.8 mL, 0.01 M) and sodium citrate (0.5 mL, 0.01M) were added to 40 mL of deionized H_2O with continuous stirring. Next, freshly prepared $NaBH_4$ (0.12 mL, 0.1M) was added and when the solution changed from colorless to light pink / orange (approximately 30 minutes), stirring was stopped and the solution was left undisturbed for 2 h. Star shape GN-particles (GNS, Figure 1B) were synthesized using a two-step procedure as reported (51). The first step involved synthesis of small size spherical GN-particle seed as described above for GNP, followed by the addition of shape-templating surfactant cetyltrimethylammonium bromide (46.88 mL, 0.59 mM) and 0.3 mL, 0.01 M $AgNO_3$ and incubation for 24 hours to synthesize GNS (53, 55). Cage shape GN-particles (GNC, Figure 1C) were prepared by galvanic replacement reaction (53, 55). Initially silver nanocubes were synthesized followed by the addition of $HAuCl_4.3H_2O$ (5 mL, 0.01M) to 5 mL of concentrated silver nanocubes (0.01mM). The mixture was dissolved in 70 ml nanopure water and boiled for few minutes. Triangular GN-prisms (NPR, Figure 1D) were prepared using a two-step seed mediated procedure as reported (54). In brief, $HAuCl_4.3H_2O$ (5 mL, 0.01M) solution was mixed with $AgNO_3$ (10 mL, 0.0029M) and trisodium citrate (10 mL, 0.0025M) and cooled in an ice bath for 3–4 hours. After that an aqueous solution of $NaBH_4$ (0.1 M) was added drop by drop with vigorous stirring followed by addition of aqueous poly(N-vinyl-2-pyrrolidone) (PVP) solution (10 mL, 0.002M) with vigorous stirring. The size and shape of GN-particles were characterized using the high-resolution tunneling electron microscope (HRTEM) (Figure 1) and dynamic light scattering (DLS) measurement using Nano instrument from Malvern Zetasizer (Table 1).

2.3. Synthesis of antigen conjugated GN-particles

Covalent immobilization of the CHrPfs25 antigen onto the GN-particles was performed using 4-amino-thio phenol (4-ATP) and a glutaraldehyde spacer method (51–53). In brief, 10 mM 4-ATP added to 20 mL of GN-particles and the solution was kept at 55°C for 6 hours under constant sonication and excess ATP was removed by centrifugation at 8,000 rpm for 30 minutes. In the next step 15 mL of amine-functionalized GN-particles were

dispersed into 0.01 M PBS containing 5% glutaraldehyde and CHrPfs25 antigen for 12 h. The CHrPfs25-modified GN-particles were washed with PBS to remove excess antigen. In addition to covalent immobilization, we also evaluated CHrPfs25 admixed 1 hour prior to immunization with GN particles. To avoid nonspecific interactions, we also tested GN particles coated with thiolated polyethylene glycol (SH-PEG). For developing PEG coated gold nanoparticles, different shape nanoparticles were treated with (10^{-4} M) polyethylene glycol (PEG) thiol acid (Sigma & Aldrich) for 6 hours at room temperature. We have used Au-S chemistry to coat PEG on GN particles. DLS (Table 1) and TEM (Figure 1) characterization confirmed no significant changes in shape and the size of GN-particles after conjugation with PEG and antigen. To make sure nanoparticles are not aggregated with time, we have performed DLS measurements at various time points, and we have noticed that GN particles remain stable even after 6 months.

2.4. Animal immunizations

Four to five weeks old female BALB/c mice were immunized with 10 μg of CHrPfs25 and various GN-particles. Four groups of mice (n=5) were immunized with Pfs25 conjugated with GNP and GNS with or without alum adjuvant. An additional six groups of mice (n=4) were immunized with CHrPfs25 ad-mixed with GNP, GNC, and NPR with or without coating with SH-PEG. All the groups of mice were vaccinated through intramuscular (IM) route (quadriceps) in a total volume of 0.1mL. Mice were boosted with the same amount of CHrPfs25 antigen in respective GN-particles at 3 week intervals and bled on day 21, 31 and 52 to collect sera for analysis.

2.5. Antibody end-point titers and isotypes by ELISA

Antibody end-point titers and IgG isotypes were determined by ELISA (24). IgG isotypes were analyzed by ELISA. After incubation with purified IgG (100 ng/ml) from immunized mice sera were incubated with HRP-conjugated anti-mouse IgG1, IgG2a, IgG2b and IgG3 (Life Technologies, CA) prior to color development and absorbance measurement.

2.6. Purification of total IgG

Purification of total IgG was accomplished using Protein A-Sepharose beads as reported (24). Briefly, pooled sera were diluted (1:1) with the binding buffer (1.5M glycine, 3M NaCl, pH 9.0) and then incubated for 2 hours at 4°C with pre-equilibrated Protein A-Sepharose beads on a rocker. The beads were packed in a column and washed with the binding buffer until no protein was detected (A_{280} by nanodrop) in the washes. The bound IgG was eluted with 0.2M glycine (pH 2.5) in tubes containing 50 μl 1M Tris-HCl, pH 9.0 followed by buffer exchange using PBS (pH 7.4). BCA protein assay kit (Thermo Scientific, Rockford, IL) was used to determine the concentration of total IgG.

2.7. Membrane feeding assay

Four different concentrations (400, 200, 100, 50 μg/mL) of total IgG were tested in standard membrane feeding assay (MFA) to determine the transmission blocking efficacy of antibodies (24). Briefly, 25–30 starved (4 hours) female *An. gambiae* (Keele strain) mosquitoes (4–6 days old adult) were fed with cultured *P. falciparum* (NF54) gametocytes

(0.3% final gametocytemia) diluted with normal human serum (NHS) and human erythrocytes to ~50% final heamatocrit and purified IgG from adjuvant alone immunized mice sera or from test sera using mini glass feeders, warmed to 37°C using a circulating water bath. Mosquitoes were allowed to feed for 15 minutes and blood-fed mosquitoes were maintained for 8–9 days at 26°C and 60–80% relative humidity. Evaluation of infectivity prevalence and transmission blocking activity was determined by counting the number of oocysts in the mosquito midguts.

2.8. Statistical analysis

Antibody endpoint antibody titer was defined as serum dilutions giving an absorbance higher than the mean absorbance of pre-immune serum + 3SD. GraphPad Instat3 software package was used for statistical analysis. Percent reduction in oocyst development in the mosquitoes was calculated using the formula [100× (mean oocyst number in negative control − mean oocyst number in test)/mean oocyst number in negative control]. One way analysis of variance (ANOVA) Kruskal-Wallis test was used to assess statistical significance. *P* values of <0.05 were considered significant.

3. Results

3.1. Qualitative and quantitative analysis of CHrPfs25 protein and stability

Pfs25 contains eleven disulfide bonds, critical for the functional immunogenicity, thus, mis-pairing of cysteine residues leads to mis-folding/aggregation resulting in low yields of bioactive recombinant protein (21, 22, 24). In order to establish reproducibility of CHrPfs25 purification, three independent batches of CHrPfs25 were produced at different times to analyze the quality and quantity. The purified protein was monomeric as revealed by denaturing non-reducing SDS-PAGE and recognized by Pfs25-specific monoclonal antibody ID3 under non-reduced SDS-PAGE condition. The yield of protein varied between 3 and 8 mg/mL. All three batches of CHrPfs25 were stored at 4°C in PBS and assessed by SDS-PAGE and western blotting after 4 and 18 months. No aggregation and degradation of protein was detected suggesting long term stability of purified protein at 4°C. Moreover, the protein stored for up to 18 months at 4°C retained the reduction-sensitive conformational epitopes (data not shown).

3.2. Physicochemical characterization of GN-particles

GN-particles exhibit unique physicochemical properties including surface charges and ability to bind amine and thiol groups, which allow surface modifications. The shapes of GNP, GNS, GNC and NPR were determined by high-resolution tunneling electron microscope (HRTEM) (Fig. 1) and the average size before conjugation with CHrPfs25 antigen was 30, 50, 60, and 30–40 nm, respectively (Table 1). After conjugation/attachment of the antigen, the size of GNP (45±4nm), GNS (64±5nm), GNC (73±5nm) and NPR (48±8nm) was found to increase slightly. Surface charge measured as zeta potential also showed increased negative values after conjugation of protein. GNS showed the highest zeta potential (−1.12 mV), while GNP had the lowest (−6.12 mV) value. The overall protein binding capacity on the surface of GN-particles was estimated using fluorophore attached protein molecule (50–55). The bound protein was detached from GN-particles using KCN

and quantified by measuring fluorescence. The average number of protein molecules bound to different GN-particles was estimated to be 600, 750, 900 and 450 for GNP, GNS, GNC and NPR, respectively. To improve the stability of antigen conjugated with GN-particles in biological medium, and to prevent non-specific charge-charge interactions between the surface of GN-particles and target antigen, GN-particles coated with SH-PEG were also tested. TEM analysis showed no morphology changes after PEG conjugation (not shown).

3.3. Stability of CHrPfs25 after conjugation with gold-nanoparticles

Conformational integrity of CHrPfs25 after conjugation of Pfs25 on the surface of GN-particles was established to assess the quality of the protein and the integrity of reduction-sensitive epitopes. The protein molecules were detached from the surface of GN-particles by using SDS and analyzed by non-reducing SDS-PAGE and western blot analysis using monoclonal antibody ID3 (as in 3.1). The detached protein remained monomeric and retained epitopes recognized by Pfs25-specific monoclonal antibody ID3, suggesting that the quality and conformational integrity of protein was not affected after attachment with GN-particles (data not shown).

3.4. Analysis of antibody responses after immunization with antigen delivered with GN-particles

GN-particles of different shapes, sizes and physicochemical properties were used to assess impact on immunogenicity outcomes. Initially, antibody responses in mice immunized with CHrPfs25 conjugated with GNP or GNS with or without alum adjuvant were evaluated (Table 2A). Pfs25 antigen was strongly immunogenic in mice delivered with both GNP and GNS and antibody titers were significantly boosted after final dose of vaccine delivered in respective GN-particles with or without alum adjuvant. The Pfs25 conjugated with GNP and GNS and administered with or without alum elicited comparable antibody titers approaching 1:640,000 (Table 2a). Immunization with Pfs25 in alum by IM and IP routes has previously revealed similar antibody titers (56). Similarly, Pfs25 admixed with GNP, NPR and GNC also induced high antibody titers of 1:1,280,000, 1:640,000 and 1: 320,000, respectively (Table 2b). In contrast, Pfs25 administered using SH-PEG coated GNP, GNC and NPR revealed 2 to 10-fold reduced antibody titers with average antibody titers of 1:110,000, 1:130,000 and 1:260,000, respectively (Table 2b). Mice immunized with mixture of GN-particles alone, with or without alum adjuvant, did not show any antigen specific antibodies and the pooled sera were used as a negative control to determine end-point antibody titers. These studies revealed varying levels of antibody titers depending upon the shape, average size and charge on the GN-particles, with higher titers obtained when Pfs25 either conjugated or admixed with GN-particles. Moreover, GNC which has the highest protein binding capacity was not as immunogenic as GNP and GNS. Likewise SH-PEG coated GN-particles were also found to be least immunogenic of all formulations tested. Finally, combining another adjuvant like alum, did not seem to offer any further advantage.

3.5. Measurement of transmission blocking efficacy of antibodies in the immune sera from mice immunized with Pfs25 in various GN-particles

Next, we tested the transmission blocking activity of antibodies in immunized mice sera by standard MFA. Purified total IgG from immunized and control sera were used to evaluate

the transmission blocking efficacy of antibodies. Four concentrations (400, 200, 100 and 50 μg/mL) of total IgG were tested in MFA using female *An. gambiae* (Fig. 2a & b). Normal human serum (NHS) and purified IgG from adjuvant alone group were used as controls. At the highest concentration, 400 μg/mL total IgG exhibited >99% transmission blocking efficacy in all the immunization groups (Fig 2a). IgG from conjugated GNP and GNS groups with or without alum showed 98% and 82%, respectively inhibition in oocyst development (Fig 2a, panels A and B). Even when tested at 200 μg/mL concentration, total IgG from various immunization groups continued to show 83–97% inhibition of oocyst development (Fig. 2a, panels A, C and D), the only exception being conjugated GNS which revealed reduced transmission blocking activity (57 %) especially in the alum group (Fig. 2a, panel B). IgG dose dependent inhibition of oocyst development was further evident when lower concentrations (100 and 50 ug/mL) were tested in MFA (Fig. 2b). Comparison of oocyst reduction at 50 μg/mL IgG among different GN-particles and formulation groups revealed higher functional activity of IgG from NPR groups with (53% inhibition) or without HS-PEG coating (59% inhibition) as compared to other immunization groups (Fig. 2b, panels AD). These results demonstrated potency and antibody dose-dependent transmission blocking activity across various GN-particle types employed. It is worth noting that the blocking activities observed with GNP and NPR were within the similar range of IgG concentration as seen earlier with alum and other adjuvants tested (24, 56).

3.6. Evaluation of IgG isotypes

Since antibody titers and transmission blocking assays showed differences with various GN-particles, we went on to analyze isotypes of elicited IgG to seek a correlation between immunoglobulin isotypes and functional immunogenicity. Antibody response consisted of IgG1, IgG2a and IgG2b isotypes with no detectable IgG3 isotype with IgG1 being dominant. IgG isotypes were expressed as a ratio of IgG1: (IgG2a+IgG2b) to compare between different groups (Table 3). GNP and GNC revealed a strong Th1 biased IgG isotype distribution even when GNP was tested in the presence of alum which is otherwise a known Th2 biased adjuvant. Our own studies with Pfs25 in alum also demonstrated a strong Th2-biased IgG isotype distribution (Table 3). Additionally, higher ratio values obtained with GNS and NPR demonstrated a sharp contrast with GNP and GNC.

4. Discussion

The need for an effective malaria vaccine is well recognized by all stakeholders who recognize the severe consequences of the infection especially in endemic countries. Vaccines to interrupt the transmission cycle provide a useful approach in addition to targeting the infection process. However, there are several hurdles in the development of effective vaccine which needs a systematic evaluation. Constraints of making and producing a recombinant protein closely related to native conformation seems to be a critical factor in obtaining potent antibody responses with transmission blocking activity (21). The paucity of safe and effective licensed vaccine delivery and adjuvant systems presents additional challenges(35). Although many adjuvants have been evaluated in pre-clinical and investigational clinical trials, only aluminum salts (alum) and oil-in-water emulsion (MF59) are licensed for use in humans as vaccine adjuvants (57, 58). Moreover, alum is known to be

a relatively weak adjuvant for recombinant vaccine antigens and exhibits a Th2 bias, in general. Therefore, judicious combinations of recombinant protein maintaining appropriate structural conformation and an effective vaccine delivery system/adjuvant need to be developed and evaluated for eliciting effective immune responses.

In our ongoing efforts focusing on the development of potent TBV, we have previously reported on the production of CHrPfs25 in *E. coli*, in monomeric form retaining reduction-sensitive conformational epitopes of transmission blocking antibodies (24). Further evaluation of immunogenicity using standard adjuvants (CFA, alum and Montanide ISA-51) revealed strong transmission blocking responses elicited by Pfs25 administered by IP route. Seeking to further optimize and enhance immunogenicity of Pfs25 and to identify safer and effective vaccine carriers, GN-particles of various physico-chemical properties were investigated as vaccine carriers to administer CHrPfs25 *via* IM route of immunization. Results of immunogenicity data presented in Table 2 suggest a few interesting differences among various GN-particles. A single dose immunization with Pfs25 in different GN-particles appeared to prime immune responses which after the first booster immunization revealed strong boosted responses with most GN-particle formulations except admixed formulations with GNC and NPR (Table 2a, b). A similar comparison of antibody titers after the second booster immunization clearly established strong immunogenicity of Pfs25 conjugated GN-particles (Table 2a) and CHrPfs25 admixed with GNP and NPR. Surprisingly HS-PEG-coated GN-particles were found to be less effective in generating good overall antibody titers even after a booster response and though we do not the exact reason for this lower immune response, we speculate that the steric stabilization by PEG prevents the adsorption of protein on the surface of GN-particles. Alternatively, it is possible that the hydrodynamic size of PEG coated particles is not able to deliver antigen efficiently to antigen presenting cells.

Since the structural integrity and purity of vaccine antigen plays a significant role in the induction of functionally effective antibodies (21, 24), we monitored the reproducibility, quality and stability of Pfs25 in several independent batches produced at different time points and analyzed at various time points during storage and after conjugation with GN-particles. Pfs25 contains 4 EGF-like domains formed by 11 disulfide bonds and structural integrity of conformational epitopes is absolutely critical for the functional immunogenicity (21). Our results firmly established the batch to batch reproducibility of purified CHrPfs25. i.e. monomeric form in non-reducing denaturing SDS-PAGE and recognition by reduction-sensitive conformational epitope specific monoclonal antibodies even after a prolonged (up to 18 months) period of storage at 4°C. We also investigated whether the protein after conjugation with GN-particles retained functional conformation. Protein molecules detached from various GN-particles analyzed by SDS-PAGE were monomeric and Pfs25-specific monoclonal antibodies recognized the non-reduced form of detached protein. Thus, our data suggest that immunologically relevant epitopes of Pfs25 were retained even after conjugation with GN-particles.

Because specificity and potency of immune response depends on the physicochemical properties of vaccine vehicles (35, 59), various GN-particles were characterized prior to vaccinating mice. TEM and polydispersity analysis showed that size and zeta potential of

evaluated GN-particles increased slightly after conjugation/admixed with Pfs25 protein without significant changes in the overall morphology. GNC (60 nm) showed highest protein binding (approximately 900 molecules/particles) followed by GNS (50 nm), GNP (30 nm) and NPR (30–40 nm). Thus the number of estimated protein molecules attached per particle varies with the physicochemical properties and the size of the GN-particles. Since different amino acids in a protein molecule display different outcome upon covalent binding to PEG (60–62), SH-PEGylated GN-particles were used to improve the stability of particles and specific interaction of antigen with GN particles. PEG provides stability to the biological molecule *via* decreasing the zeta potential and preventing agglomeration caused by nonspecific adsorption of proteins or salts *in vivo* (63). While the morphology of particles was not changed after coating with SH-PEG, the overall immunogenicity outcomes were greatly different whether Pfs25 was conjugated or mixed with GN-particles.

Antibody mediated transmission blocking efficacy was evaluated in mosquito (*An. gambiae*) membrane feeding assays using purified total IgG from pooled immune mice sera and our studies sought to seek correlation with IgG isotypes. At the highest concentration (400 μg/mL) IgG from mice immunized with different GN-particles showed highly potent blocking regardless of IgG isotype differences. It was interesting to note that Pfs25 delivery with GNP and GNC revealed a strong Th1 biased IgG isotype distribution. This bias persisted even when GNP was tested in the presence of alum which is otherwise a known Th2 biased adjuvant. Additionally, higher IgG1/(IgG2a+IgG2b) values obtained with GNS and NPR also demonstrated a sharp contrast with GNP and GNC thus establishing immunogenicity differences among GN-particles of varying physico-chemical properties, shape and size. Transmission blocking assays also revealed relatively higher blocking with NPR when compared across other GN-particles at lower IgG concentrations (100 and 50 μg/mL). These differences thus identify further qualitative differences that can result from using different GN-particles which may differ in the uptake and presentation of antigen to antigen presenting cells. It is well established that the epitopes recognized by Pfs25-specific transmission blocking antibodies are reduction sensitive conformational in nature (21, 22). The fact that sera from mice immunized with Pfs25 and various gold nanoparticles were potent blockers in mosquito membrane feeding assays demonstrates that such functional conformational epitopes were efficiently presented to the immune system. Using the polyclonal sera, it is not possible to comment whether the repertoire of antibodies differed among different gold nanoparticle immunization groups. Finally, even though our studies revealed predominance of certain IgG isotype with different gold nanoparticles, the transmission blocking activity was not affected.

We have shown that CHrPfs25 admixed with gold nanoparticles provides an effective approach to improve immunogenicity. It may be due to the fact that antigen and nanoparticles are co-ingested by the immune cell. Our results also demonstrate that non-attachment approach also has good potential through simple mixing of nanoparticle and adjuvant, which has also been observed by other investigators (64, 65). Reported data indicate that CHrPfs25 admixed spherical gold nanoparticles (GNP) were more effective than other shapes. It can be due to the fact that, as shown in Table 1, spherical GNP are more negatively charged as compared to the other shape particles. Due to the electrostatic

interaction with cell membranes, aggregation on the cell surface will be minimum for spherical gold nanoparticle as compared to the particles of other shapes tested. As a result cellular uptake will be better for spherical GNPs. Reported data in Table 2B, indicate that PEG-coated NPs were less effective than without PEG. This can be due to the fact that PEG chain increased the particle size potentially resulting in reduced cellular uptake. Similar finding was observed by Cruz et.al. where reported data show that PEG chains cannot be extended without compromising the efficacy of targeted delivery (66). Although our data and those of others indicate nanoparticle mediated vaccines have good potential as delivery vehicles to improve vaccine immunogenicity significantly, fundamental understanding of how the size, shape and surface charge affect immunogenicity efficiency needs to be understood before they can move to the clinical practice. We need to understand how the physical and chemical properties influence nanoparticle interactions with cell, tissues and to whole body, which will be crucial to accelerate the development process of suitable nanoparticles for pharmaceutical applications.

Development of prophylactic and therapeutic vaccines using nanotechnology, “nanovaccinology” is an emerging and exponentially growing field. It offers an effective way to develop and deliver immunogenic vaccines with the possibility of targeted delivery to slow release kinetics, if desired (65). Use of gold nanoparticles offers an opportunity to evaluate particles of different shapes and size, with or without surface modifications (67). The current study presents the characterization and immunogenicity of Pfs25 and GN-particles. The data suggest that the functional immunogenicity is dependent on the shape, size and other physic-chemical properties of GN-particles tested. Therefore, GN-particles offer the potential to develop safe, highly effective and well characterized vaccine delivery carriers. The reproducibility of protein production, stability of protein for more than 18 months at 4°C and potent transmission blocking activity demonstrated by CHrPfs25 favors further development of GMP compliant nanovaccines based on Pfs25 for evaluation in phase I clinical trials in human volunteers.

Acknowledgments

These studies were supported by NIH grants R21-AI101427 and RO1-AI47089.

References

1. Miotto O, Almagro-Garcia J, Manske M, Macinnis B, Campino S, Rockett K, et al. Multiple populations of artemisinin-resistant Plasmodium falciparum in Cambodia. Nat Genet. 2013; 45:648–55. [PubMed: 23624527]
2. Ariey F, Witkowski B, Amaratunga C, Beghain J, Langlois A, Khim N, et al. A molecular marker of artemisinin-resistant Plasmodium falciparum malaria. Nature. 2014; 505:50–5. [PubMed: 24352242]
3. The RTS SCTP. First results of 3 trial of RTS,S/AS01 malaria vaccine in African children. N Engl J Med. 2011; 365:1863–75. [PubMed: 22007715]
4. The Rts SCTP. Efficacy and Safety of the RTS,S/AS01 Malaria Vaccine during 18 Months after Vaccination: A Phase 3 Randomized, Controlled Trial in Children and Young Infants at 11 African Sites. PLoS medicine. 2014; 11(7):e1001685. [PubMed: 25072396]
5. Kaslow DC. Transmission-blocking vaccines: Uses and current status of development. International Journal for Parasitology. 1997; 27(2):183–9. [PubMed: 9088989]

6. Kumar N. A vaccine to prevent transmission of human malaria: a long way to travel on a dusty and often bumy road. Current science. 2007; 92(11):1535–44.
7. Pradel G. Proteins of the malaria parasite sexual stages: expression, function and potential for transmission blocking strategies. Parasitology. 2007; 134(14):1911–29. [PubMed: 17714601]
8. Nunes JK, Woods C, Carter T, Raphael T, Morin MJ, Diallo D, et al. Development of a transmission-blocking malaria vaccine: Progress, challenges, and the path forward. Vaccine. 2014; 32(43):5531–9. [PubMed: 25077422]
9. Carter R, Gwadz RW, McAuliffe FM. Plasmodium gallinaceum: Transmission-blocking immunity in chickens: I. Comparative immunogenicity of gametocyte- and gamete-containing preparations. Experimental Parasitology. 1979; 47(2):185–93. [PubMed: 437016]
10. Gwadz R. Successful immunization against the sexual stages of Plasmodium gallinaceum. Science. 1976; 193:1150–1. [PubMed: 959832]
11. Williamson KC, Keister DB, Muratova O, Kaslow DC. Recombinant Pfs230, a Plasmodium falciparum gametocyte protein, induces antisera that reduce the infectivity of Plasmodium falciparum to mosquitoes. Molecular and Biochemical Parasitology. 1995; 75(1):33–42. [PubMed: 8720173]
12. Gerloff DL, Creasey A, Maslau S, Carter R. Structural models for the protein family characterized by gamete surface protein Pfs230 of Plasmodium falciparum. Proceedings of the National Academy of Sciences of the United States of America. 2005; 102(38):13598–603. [PubMed: 16155126]
13. Carter R, Coulson A, Bhatti S, Taylor BJ, Elliott JF. Predicted disulfide-bonded structures for three uniquely related proteins of Plasmodium falciparum, Pfs230, Pfs4845 and Pf12. Molecular and biochemical parasitology. 1995; 71(2):203–10. [PubMed: 7477102]
14. Farrance CE, Chichester JA, Musiychuk K, Shamloul M, Rhee A, Manceva SD, et al. Antibodies to plant-produced Plasmodium falciparum sexual stage protein Pfs25 exhibit transmission blocking activity. Human vaccines. 2011; 7(sup1):191–8. [PubMed: 21266847]
15. Farrance CE, Rhee A, Jones RM, Musiychuk K, Shamloul M, Sharma S, et al. A Plant-Produced Pfs230 Vaccine Candidate Blocks Transmission of Plasmodium falciparum. Clinical and Vaccine Immunology. 2011; 18(8):1351–7. [PubMed: 21715576]
16. Tachibana M, Wu Y, Iriko H, Muratova O, MacDonald NJ, Sattabongkot J, et al. N-Terminal Prodomain of Pfs230 Synthesized Using a Cell-Free System Is Sufficient To Induce Complement-Dependent Malaria Transmission-Blocking Activity. Clinical and Vaccine Immunology. 2011; 18(8):1343–50. [PubMed: 21715579]
17. Quakyi IA, Carter R, Rener J, Kumar N, Good MF, Miller LH. The 230-kDa gamete surface protein of Plasmodium falciparum is also a target for transmission-blocking antibodies. J Immunol. 1987; 139(12):4213–7. [PubMed: 2447164]
18. Rener J, Graves P, Carter R, Williams J, Burkot T. Target antigens of transmission-blocking immunity on gametes of Plasmodium falciparum. J Exp Med. 1983; 158:976–81. [PubMed: 6350527]
19. Outchkourov NS, Roeffen W, Kaan A, Jansen J, Luty A, Schuiffel D, et al. Correctly folded Pfs48/45 protein of Plasmodium falciparum elicits malaria transmission-blocking immunity in mice. Proceedings of the National Academy of Sciences. 2008; 105(11):4301–5.
20. Chowdhury DR, Angov E, Kariuki T, Kumar N. A Potent Malaria Transmission Blocking Vaccine Based on Codon Harmonized Full Length *Pfs48/45* Expressed in *Escherichia coli*. PloS one. 2009; 4(7):e6352. [PubMed: 19623257]
21. Kaslow DC, Bathurst IC, Lensen T, Ponnudurai T, Barr PJ, Keister DB. Saccharomyces cerevisiae recombinant Pfs25 adsorbed to alum elicits antibodies that block transmission of Plasmodium falciparum. Infection and immunity. 1994; 62(12):5576–80. [PubMed: 7960139]
22. Barr PJ, Green KM, Gibson HL, Bathurst IC, Quakyi IA, Kaslow DC. Recombinant Pfs25 protein of Plasmodium falciparum elicits malaria transmission-blocking immunity in experimental animals. J Exp Med. 1991; 174(5):1203–8. [PubMed: 1940798]
23. Kumar R, Nyakundi R, Kariuki T, Ozwara H, Nyamongo O, Mlambo G, et al. Functional evaluation of malaria Pfs25 DNA vaccine by in vivo electroporation in olive baboons. Vaccine. 2013; 31(31):3140–7. [PubMed: 23684840]

24. Kumar R, Angov E, Kumar N. Potent Malaria Transmission-Blocking Antibody Responses Elicited by Plasmodium falciparum Pfs25 Expressed in Escherichia coli after Successful Protein Refolding. Infection and immunity. 2014; 82(4):1453–9. [PubMed: 24421036]
25. Lobo CA, Dhar R, Kumar N. Immunization of Mice with DNA-Based Pfs25 Elicits Potent Malaria Transmission-Blocking Antibodies. Infection and immunity. 1999; 67(4):1688–93. [PubMed: 10085005]
26. Tsuboi T, Takeo S, Iriko H, Jin L, Tsuchimochi M, Matsuda S, et al. Wheat Germ Cell-Free System-Based Production of Malaria Proteins for Discovery of Novel Vaccine Candidates. Infection and immunity. 2008; 76(4):1702–8. [PubMed: 18268027]
27. Gregory JA, Li F, Tomosada LM, Cox CJ, Topol AB, Vinetz JM, et al. Algae-Produced Pfs25 Elicits Antibodies That Inhibit Malaria Transmission. PloS one. 2012; 7(5):e37179. [PubMed: 22615931]
28. Wu Y, Przysiecki C, Flanagan E, Bello-Irizarry SN, Ionescu R, Muratova O, et al. Sustained high-titer antibody responses induced by conjugating a malarial vaccine candidate to outer-membrane protein complex. Proceedings of the National Academy of Sciences. 2006; 103(48):18243–8.
29. Kubler-Kielb J, Majadly F, Wu Y, Narum DL, Guo C, Miller LH, et al. Long-lasting and transmission-blocking activity of antibodies to Plasmodium falciparum elicited in mice by protein conjugates of Pfs25. Proceedings of the National Academy of Sciences. 2007; 104(1):293–8.
30. Shimp RL Jr, Rowe C, Reiter K, Chen B, Nguyen V, Aebig J, et al. Development of a Pfs25-EPA malaria transmission blocking vaccine as a chemically conjugated nanoparticle. Vaccine. 2013; 31(28):2954–62. [PubMed: 23623858]
31. Jones RM, Chichester JA, Mett V, Jaje J, Tottey S, Manceva S, et al. A Plant-Produced Pfs25 VLP Malaria Vaccine Candidate Induces Persistent Transmission Blocking Antibodies against *Plasmodium falciparum* in Immunized Mice. PloS one. 2013; 8(11):e79538. [PubMed: 24260245]
32. Wu Y, Ellis RD, Shaffer D, Fontes E, Malkin EM, Mahanty S, et al. Phase 1 Trial of Malaria Transmission Blocking Vaccine Candidates Pfs25 and Pvs25 Formulated with Montanide ISA 51. PloS one. 2008; 3(7):e2636. [PubMed: 18612426]
33. Kaslow DC, Quakyi IA, Syin C, Raum MG, Keister DB, Coligan JE, et al. A vaccine candidate from the sexual stage of human malaria that contains EGF-like domains. Nature. 1988; 333(6168): 74–6. [PubMed: 3283563]
34. Saxena AK, Singh K, Hua-Poo S, Klein MM, Stowers AW, Saul AJ, et al. The essential mosquito-stage P25 and P28 proteins from Plasmodium form tile-like triangular prisms. Nature Structural & Molecular Biology. 2006; 13(1):90–1.
35. Reed SG, Orr MT, Fox CB. Key roles of adjuvants in modern vaccines. Nat Med. 2013; 19(12): 1597–608. [PubMed: 24309663]
36. de Jong S, Chikh G, Sekirov L, Raney S, Semple S, Klimuk S, et al. Encapsulation in liposomal nanoparticles enhances the immunostimulatory, adjuvant and anti-tumor activity of subcutaneously administered CpG ODN. Cancer Immunology, Immunotherapy. 2007; 56(8): 1251–64. [PubMed: 17242927]
37. Beaudette TT, Bachelder EM, Cohen JA, Obermeyer AC, Broaders KE, Fréchet JMJ, et al. In Vivo Studies on the Effect of Co-Encapsulation of CpG DNA and Antigen in Acid-Degradable Microparticle Vaccines. Molecular Pharmaceutics. 2009; 6(4):1160–9. [PubMed: 19415922]
38. Shukla R, Bansal V, Chaudhary M, Basu A, Bhonde RR, Sastry M. Biocompatibility of Gold Nanoparticles and Their Endocytotic Fate Inside the Cellular Compartment: A Microscopic Overview. Langmuir. 2005; 21(23):10644–54. [PubMed: 16262332]
39. Ghosh P, Han G, De M, Kim CK, Rotello VM. Gold nanoparticles in delivery applications. Advanced drug delivery reviews. 2008; 60(11):1307–15. [PubMed: 18555555]
40. Bastús NG, Sánchez-Tilló E, Pujals S, Farrera C, Kogan MJ, Giralt E, et al. Peptides conjugated to gold nanoparticles induce macrophage activation. Molecular Immunology. 2009; 46(4):743–8. [PubMed: 18996597]
41. Bastús NG, Sánchez-Tilló E, Pujals S, Farrera C, López C, Giralt E, et al. Homogeneous Conjugation of Peptides onto Gold Nanoparticles Enhances Macrophage Response. ACS Nano. 2009; 3(6):1335–44. [PubMed: 19489561]

42. Rana S, Bajaj A, Mout R, Rotello VM. Monolayer coated gold nanoparticles for delivery applications. Advanced drug delivery reviews. 2012; 64(2):200–16. [PubMed: 21925556]
43. Sau TK, Murphy CJ. Room Temperature, High-Yield Synthesis of Multiple Shapes of Gold Nanoparticles in Aqueous Solution. Journal of the American Chemical Society. 2004; 126(28): 8648–9. [PubMed: 15250706]
44. Perrault SD, Chan WCW. Synthesis and Surface Modification of Highly Monodispersed, Spherical Gold Nanoparticles of 50 200 nm. Journal of the American Chemical Society. 2009; 131(47): 17042–3. [PubMed: 19891442]
45. Villiers C, Freitas H, Couderc R, Villiers M-B, Marche P. Analysis of the toxicity of gold nano particles on the immune system: effect on dendritic cell functions. Journal of Nanoparticle Research. 2010; 12(1):55–60. [PubMed: 21841911]
46. Arnáiz B, Martínez-Ávila O, Falcon-Perez JM, Penadés S. Cellular Uptake of Gold Nanoparticles Bearing HIV gp120 Oligomannosides. Bioconjugate Chemistry. 2012; 23(4):814–25. [PubMed: 22433013]
47. Chen Y-S, Hung Y-C, Liau I, Huang G. Assessment of the In Vivo Toxicity of Gold Nanoparticles. Nanoscale Research Letters. 2009; 4(8):858–64. [PubMed: 20596373]
48. Chen YSHYC, Lin WH, Huang GS. Assessment of gold nanoparticles as a size-dependent vaccine carrier for enhancing the antibody response against synthetic foot-and-mouth disease virus peptide. Nanotechnology. 2010; 21(19):8.
49. Brito LA, Singh M. Acceptable levels of endotoxin in vaccine formulations during preclinical research. Journal of pharmaceutical sciences. 2011; 100(1):34–7. [PubMed: 20575063]
50. Dasary SSR, Singh AK, Senapati D, Yu H, Ray PC. Gold Nanoparticle Based Label-Free SERS Probe for Ultrasensitive and Selective Detection of Trinitrotoluene. Journal of the American Chemical Society. 2009; 131(38):13806–12. [PubMed: 19736926]
51. Lu W, Singh AK, Khan SA, Senapati D, Yu H, Ray PC. Gold Nano-Popcorn-Based Targeted Diagnosis, Nanotherapy Treatment, and In Situ Monitoring of Photothermal Therapy Response of Prostate Cancer Cells Using Surface-Enhanced Raman Spectroscopy. Journal of the American Chemical Society. 2010; 132(51):18103–14. [PubMed: 21128627]
52. Singh AK, Khan SA, Fan Z, Demeritte T, Senapati D, Kanchanapally R, et al. Development of a Long-Range Surface-Enhanced Raman Spectroscopy Ruler. Journal of the American Chemical Society. 2012; 134(20):8662–9. [PubMed: 22559168]
53. Demeritte T, Fan Z, Sinha SS, Duan J, Pachter R, Ray PC. Gold Nanocage Assemblies for Selective Second Harmonic Generation Imaging of Cancer Cell. Chemistry – A European Journal. 2014; 20(4):1017–22.
54. Singh AK, Senapati D, Neely A, Kolawole G, Hawker C, Ray PC. Nonlinear optical properties of triangular silver nanomaterials. Chemical Physics Letters. 2009; 481(1–3):94–8.
55. Kanchanapally R, Sinha SS, Fan Z, Dubey M, Zakar E, Ray PC. Graphene Oxide–Gold Nanocage Hybrid Platform for Trace Level Identification of Nitro Explosives Using a Raman Fingerprint. The Journal of Physical Chemistry C. 2014; 118(13):7070–5.
56. Kumar R, Ledet G, Graves R, Datta D, Robinson S, Bansal G, et al. Potent Functional Immunogenicity of Plasmodium falciparum Transmission-Blocking Antigen (Pfs25) Delivered with Nanoemulsion and Porous Polymeric Nanoparticles. Pharm Res. 2015:1–10. [PubMed: 25168518]
57. Kenney JS, Hughes BW, Masada MP, Allison AC. Influence of adjuvants on the quantity, affinity, isotype and epitope specificity of murine antibodies. Journal of Immunological Methods. 1989; 121(2):157–66. [PubMed: 2474611]
58. McKee A, MacLeod M, Kappler J, Marrack P. Immune mechanisms of protection: can adjuvants rise to the challenge? BMC Biology. 2010; 8(1):37. [PubMed: 20385031]
59. Bachmann MF, Jennings GT. Vaccine delivery: a matter of size, geometry, kinetics and molecular patterns. Nat Rev Immunol. 2010; 10(11):787–96. [PubMed: 20948547]
60. Pasut G, Veronese FM. State of the art in PEGylation: The great versatility achieved after forty years of research. Journal of Controlled Release. 2012; 161(2):461–72. [PubMed: 22094104]
61. Veronese FM, Pasut G. PEGylation, successful approach to drug delivery. Drug discovery today. 2005; 10(21):1451–8. [PubMed: 16243265]

62. Karathanasis E, Ayyagari AL, Bhavane R, Bellamkonda RV, Annapragada AV. Preparation of in vivo cleavable agglomerated liposomes suitable for modulated pulmonary drug delivery. Journal of Controlled Release. 2005; 103(1):159–75. [PubMed: 15710508]

63. Knop K, Hoogenboom R, Fischer D, Schubert US. Poly(ethylene glycol) in Drug Delivery: Pros and Cons as Well as Potential Alternatives. Angewandte Chemie International Edition. 2010; 49(36):6288–308.

64. Wibowo N, Chuan YP, Seth A, Cordoba Y, Lua LHL, Middelberg APJ. Co-administration of non-carrier nanoparticles boosts antigen immune response without requiring protein conjugation. Vaccine. 2014; 32(29):3664–9. [PubMed: 24793947]

65. Zhao L, Seth A, Wibowo N, Zhao C-X, Mitter N, Yu C, et al. Nanoparticle vaccines. Vaccine. 2014; 32(3):327–37. [PubMed: 24295808]

66. Cruz LJ, Tacken PJ, Fokkink R, Figdor CG. The influence of PEG chain length and targeting moiety on antibody-mediated delivery of nanoparticle vaccines to human dendritic cells. Biomaterials. 2011; 32(28):6791–803. [PubMed: 21724247]

67. Niikura K, Matsunaga T, Suzuki T, Kobayashi S, Yamaguchi H, Orba Y, et al. Gold nanoparticles as a vaccine platform: influence of size and shape on immunological responses in vitro and in vivo. ACS nano. 2013; 7(5):3926–38. [PubMed: 23631767]

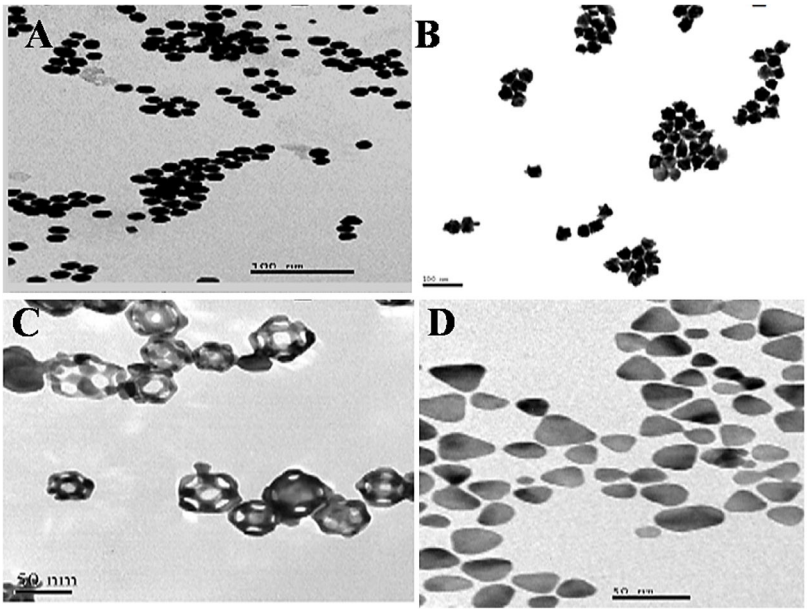

Figure 1.

Fig. 2a

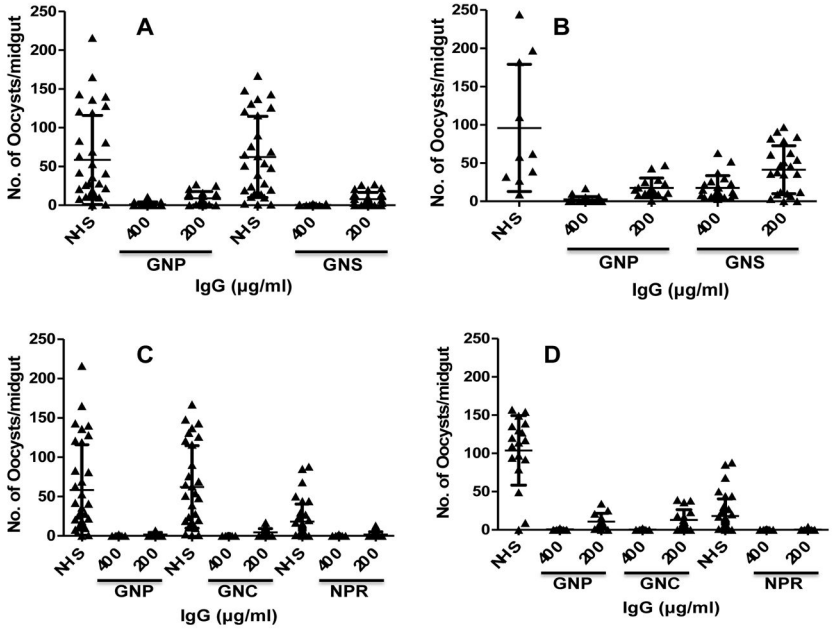

Fig. 2b

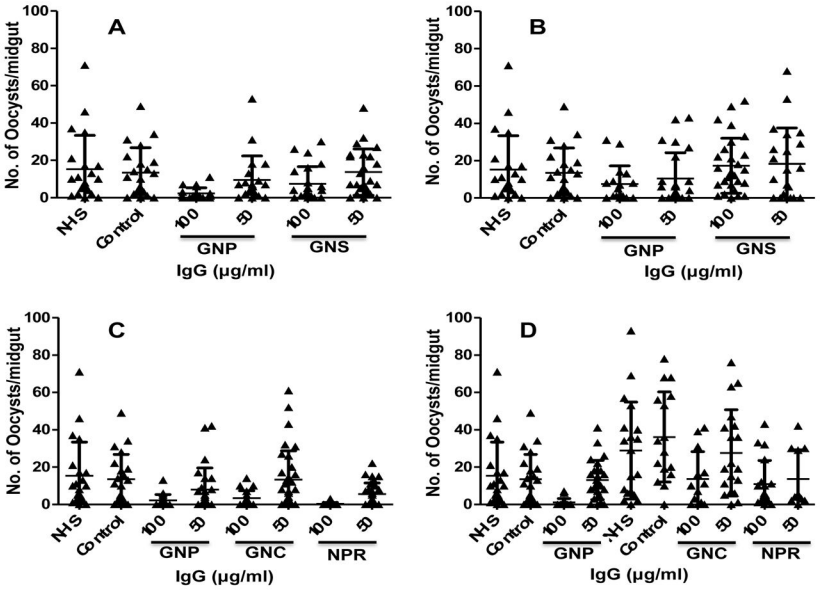

Figure 2.

Table 1

Characterization of gold nanoparticles having different sizes and shapes

Shapes	Size (nm)*		Zeta Potential (mV)*		Protein/GN particle**
	Before	After	Before	After	
Spherical (GNP)	30	45 ± 4	nm	−6.12	600
Star (GNS)	50	64 ± 5	nm	−1.12	750
Cage (GNC)	60	73 ± 5	nm	−4.38	900
Nanoprism (NPR)	30–40	48 ± 8	nm	−5.16	450

* Size and charge before and after conjugation of Pfs25, nm (not measured).

** Protein binding capacity differences were established using fluorescent labeled protein molecules.

Table 2

Anti-Pfs25 antibody end-point titers in sera from mice immunized with ChrPfs25

(a) ChrPfs25 conjugated with gold nanoparticles			
		Antibody Titers	
Groups	**Prime**	**1st Boost**	**2nd Boost**
GNP	1200	42,000	640,000
GNS	ND	103,000	640,000
GNP-Alum	1800	73,600	640,000
GNS-Alum	2300	20,200	608,000

(b) ChrPfs25 admixed with gold nanoparticles			
		Antibody Titers	
Groups	**Prime**	**1st Boost**	**2nd Boost**
GNP	3600	40,000	1280,000
GNC	125	1125	320,000
NPR	ND	7500	640,000
GNP-PEG	125	100,000	110,000
GNC-PEG	ND	96,600	130,000
NPR-PEG	ND	12,600	260,000

ND-Not detectable

Table 3

Analysis of IgG isotypes in immune sera from mice immunized using various GN-particles and expressed as IgG1/(IgG2a+IgG2b) ratios

GN-particles	No Alum	Alum	SH-PEG Coated
GNP	0.79	1.17	
GNS	2.15	8.72	
GNP	1.03		0.63
GNC	0.96		4.34
NPR	3.25		2.23
		4.0, 12.7	

*These ratios were obtained mice immunized with ChrPfs25 in alum alone in two different experiments.